Research

Oikos 118: 641–652, 2009
doi: 10.1111/j.1600-0706.2008.17003.x,

Subject Editor: Thomas Valone. Accepted 7 November 2008

Memory keeps you at home: a mechanistic model for home range emergence

Bram Van Moorter, Darcy Visscher, Simon Benhamou, Luca Börger, Mark S. Boyce and Jean-Michel Gaillard

B. Van Moorter (bram.van.moorter@gmail.com) and J.-M. Gaillard, Unité Mixte de Recherche No. 5558 « Biométrie et Biologie Evolutive », Bâtiment 711, Univ. Claude Bernard Lyon 1, 43 Boulevard du 11 novembre 1918, FR–69622 Villeurbanne Cedex, France. Present address for BVM: Dept of Biology, NTNU, Høgskoleringen 5, NO–7491 Trondheim, Norway. – D. Visscher and M. S. Boyce, Dept of Biological Sciences, Univ. of Alberta, Edmonton, AB T6G 2E9, Canada. – S. Benhamou, Unité Mixte de Recherche No. 5175 «Ecologie Fonctionnelle et Evolutive », 1919 Route de Mende, FR–34293 Montpellier cedex 5, France. – L. Börger, Dept of Integrative Biology, Univ. of Guelph, Guelph, ON N1G 2W1, Canada.

Despite its central place in animal ecology no general mechanistic movement model with an emergent home-range pattern has yet been proposed. Random walk models, which are commonly used to model animal movement, show diffusion instead of a bounded home range and therefore require special modifications. Current approaches for mechanistic modeling of home ranges apply only to a limited set of taxa, namely territorial animals and/or central place foragers. In this paper we present a more general mechanistic movement model based on a biased correlated random walk, which shows the potential for home-range behavior. The model is based on an animal tracking a dynamic resource landscape, using a biologically plausible two-part memory system, i.e. a reference- and a working-memory. Our results show that by adding these memory processes the random walker produces home-range behavior as it gains experience, which also leads to more efficient resource use. Interestingly, home-range patterns, which we assessed based on home-range overlap and increase in area covered with time, require the combined action of both memory components to emerge. Our model has the potential to predict home-range size and can be used for comparative analysis of the mechanisms shaping home-range patterns.

Movement lies at the core of how animals interact with their environment. Most animals, including all vertebrates, move through their environment, which allows them to use resources that are heterogeneously distributed in space. However, in contrast to the large movement capacities animals possess, these movements are restricted to a limited area for a wide variety of species, including mammals (Spencer et al. 1990, Schaefer et al. 2000, Foerster and Vaughan 2002, Martinoli et al. 2006), birds (reviewed by Greenwood and Harvey 1982, Weimerskirch 2007), reptiles (Arvisais et al. 2002, Heise and Epperson 2005), amphibians (Daugherty and Sheldon 1982, Crump 1986), fish (Rodriguez 2002, Crook 2004), and insects (Switzer 1997, Mooney and Haloin 2005). This confined, temporally stable area is commonly called the home range (Burt 1943, Cooper 1978, White and Garrott 1990).

Despite the fundamental importance of home-range behavior in structuring ecological processes (Gautestad and Mysterud 2005, Rhodes 2005, Fagan et al. 2007, Wang and Grimm 2007), mechanistic home-range models of general applicability are still missing (reviewed by Börger et al. 2008). Movement models can be restrained to a limited area by either imposed limits (Folse et al. 1989) or they can show home-range patterns as an emergent property from their movement rules. Existing mechanistic movement models that lead to the emergence of home-range behavior out of potentially unrestricted movement paths apply only to central place foragers or to territorial species (reviewed by Stamps and Krishnan 1999, Moorcroft and Lewis 2006). Many animals are, however, non-territorial and home ranges are generally multinuclear (Don and Rennolls 1983).

Memory processes have been investigated as an alternative mechanism to stabilize the home range yet despite their capacity to slow down the diffusion speed, none of these models has shown a stable home range (Tan et al. 2001, 2002, Gautestad and Mysterud 2005). The continuous increase (Tan et al. 2001, Gautestad and Mysterud 2005) or drift (Tan et al. 2002) of the set of previously visited sites due to occasional movements into unfamiliar sites (Börger et al. 2008) explains the absence of a stable home range. The utility [utility is here used in the economical sense of the word; utility is the numerical measure of an individual's preference or subjective value for something (see Stephens and Krebs 1986 for applications in ecology), which is measured in 'utils'] of a site in these models simply increases due to previous visits. However, it

seems unrealistic that a site's utility should depend solely on previous visitation events. In artificial intelligence modeling of animal movements, memory has been successfully used to simulate stable home ranges in heterogeneous landscapes (Folse et al. 1989). However, in this case the increase of familiar sites was prevented by a programmed limit to the number of sites in the memory (Folse et al. 1989), thus the home range can hardly be considered an emergent property.

Most environments are spatially heterogeneous to an animal, due to differences in, for instance, resource availability or predation risk. This spatial heterogeneity in utility drives movement by animals (Bell 1991). Spatial heterogeneity can be represented using patches; a patch is "a surface area differing from its surroundings in nature or appearance" (Wiens 1979). We consider patches as areas differing from their surroundings by an elevated utility, due to, for instance, resources or protection against predators they offer. The utility of a patch for an animal usually decreases with residence time in the patch as a consequence of environmental processes like resource depletion (Charnov 1976) or increased predation risk (Mitchell and Lima 2002), or processes influencing individual motivation like satiation (Pettersson and Brönmark 1993). The idea of decreased utility has led to the development of optimal patch-leaving decisions (Charnov 1976, reviewed by Stephens and Krebs 1986). After the animal leaves a patch, however, utility in general will start to increase again as the environmental resources replenish and predation risk decreases, or individual motivation increases due to hunger.

In general, studies on animal foraging have led to a refined understanding of spatial decisions animals make to acquire resources for survival and reproduction. Animal home ranges are a spatial expression of these movements, yet current movement-based mechanistic home-range models mostly ignore this rich spatial foraging literature (Börger et al. 2008). This is a crucial limitation. For example, recent non-movement based mechanistic home-range models (Mitchell and Powell 2004, 2007) have shown that explicit considerations of patch choice behavior need to be included in mechanistic home-range models.

Two main forces can be considered governing the movement of an animal in a home range. First, the motivation to move away from the resident patch, due to its decreased utility (e.g. caused by resource consumption). Second, the motivation to return to previously visited sites following an increased expected utility of non-used patches (e.g. resource renewal). Howery et al. (1999) reviewed spatial memory as a two-part system, consisting of reference and working memory (first distinguished by Honig 1978). The reference memory stores preferences for certain feeding areas (Howery et al. 1999), whereas the working memory is used to avoid backtracking on recently depleted patches (Brown et al. 1997, Howery et al. 1999).

Here we present a home-range model based on a random walk using the attraction towards several different patches whose utility varies in time. A two-part memory system is used to model the two main forces governing the movement of an animal. Motivation to return to previously visited patches is stored in the reference memory, whereas motivation to move away from patches with lowered utility is controlled by the working memory. We investigate the temporal stability of ranges occupied by a random walk with memory in a heterogeneous environment. Because the model depends critically on the interaction between both memory types, we investigate in detail how process rates of both memory types influence emergence of stable home ranges.

Methods

The dynamic utility landscape model

The utility of patches, used by mobile foragers, shows depletion/replenishment cycles (Possingham 1988), which we modeled using well-established functions from foraging theory (Stephens and Krebs 1986). The landscape configuration, instead, was kept constant in all simulations, to avoid the potentially confounding effects of variation in landscape configuration on forager space use. The simulated landscape consisted of 250 patches of the same size (radius = 106 units) and intrinsic patch utility (maxU, Table 1), distributed randomly without overlap on a $10\,000 \times 10\,000$ unit landscape (Fig. 1), the latter set within an unlimited environment. The default step length of the forager was set to 100 units per time step (Table 1).

When a forager is in a patch, the utility of the patch decreases as a function of residence time. We modeled patch depletion using a gain function with a threshold, i.e. a constant gain curve that drops to zero when depleted (Stephen and Krebs 1986). This threshold function has the desirable property that optimal residence time is straightforward to model. Because no decrease in the gain function occurs before a patch is completely depleted, the animal should stay within the patch until its depletion. Other functions are possible (discussed by Stephens and Krebs 1986), but these will affect only the temporal dynamics of the environment, i.e. patch residence time and patch renewal speed. We investigated the effect of both parameters on our results. The default patch depletion rate (2500 'utils' per time step, Table 1) leads to complete depletion of the patch by the animal in 15 time steps (thus residence time of the forager is 15 time steps).

The utility (U) of patch (p) is replenished over time (t) when unoccupied, up to the common limit (the intrinsic patch quality, maxU), following a logistic growth function:

$$U[p]_{t+1} = U[p]_t + r \times \left(1 - \frac{U[p]_t}{\max U[p]}\right) \times U[p]_t \qquad (1)$$

With the default growth rate (r = 0.25, Table 1), a depleted patch will have replenished itself completely after 40 time steps (for the logistic growth, patch utility ranges between maxU × [0.01 and 0.99]).

The movement model

One of the most flexible ways to model animal movements is the random walk approach (Turchin 1998). Given the diffusive nature of random walks, special model features need to be included to allow for the emergence of home ranges (Solow 1990) and the biological relevance of home-range models lies in the features used to model this balance between diffusion and constraint space use. We used a biased correlated random walk model, which is a random

Table 1. Description of the parameters and variables used in the simulations. Vectors, which contain x- and y-coordinates, are represented by letters with an arrow. We provide the function (directly or as a reference to an equation in the main text) and the range of values for the variables, with the default values for the parameters, as well as the biological meaning for both.

Variables	Function	Range	Biological meaning
$U[p]_t$	Eq. 1	0.01–maxU[p]	utility of patch p
$M_W[p]_t$	Eq. 2	0.001–0.999	reference memory strength for patch p at time t
$M_R[p]_t$	Eq. 2	0.001–0.999	working memory strength for patch p at time t
$D[p]_t$	distance(current position, patch[p])	–	patch distance from the current position of the forager
$V[p]_t$	Eq. 3, 4	–	patch value
$\vec{d}[p]_t$	direction(current position, patch[p])	unit vector	direction of the patch from the current position of the forager
$\vec{v}_t$	Eq. 5	–	resultant attraction vector
$\vec{r}_t$	direction(previous, current position)	unit vector	direction taken in the previous time step

Parameters	Value range	Default value	Meaning
r	0.08, 0.125, 0.25, 0.5 and 0.75	0.25	patch utility renewal rate
maxU[p]	35299	35299	maximum patch utility
Depletion rate	500, 1500, 2500, 3500 and 4500	2500	depletion rate
r_W	0, 0.0001, 0.001, 0.005, 0.01, 0.05, 0.1, 1 and infinite	0.01	working memory decay rate
r_R	0, 0.0001, 0.001, 0.005, 0.01, 0.05, 0.1, 1 and infinite	0.0001	reference memory decay rate
cor	0, 0.2, 0.4, 0.6, 0.8 and 0.99	0.2	directional persistance
Step length	50, 100, 150, 500 and 1000	100	step length

walk where the direction of the movement is biased towards a given direction and the direction also is correlated between consecutive steps. A correlated random walk model was chosen to model the diffusive component of animal movements in a realistic way (Bovet and Benhamou 1988, Tuchin 1998). The new development of our approach is the inclusion of memory-based patch-attraction mechanisms that determine the bias to certain locations, leading thereby to the emergence of home-range behavior.

More in detail, the correlated random walk contains a positive correlation between directions of consecutive movement steps and allows us to model the short-time directional persistence characteristic of animals (Bovet and Benhamou 1988). On the other hand, the bias component works on longer time scales and directs the movement of the animal. In our model, the bias is determined by the resultant vector of attraction from the different resource patches in the landscape. The attraction of each patch is determined by the interaction of two memory mechanisms (see Table 1 for an overview of the variables and parameters used in the model). One mechanism deals with the motivation to come back to previously visited patches: the reference memory ($M_R[p]_t$), which retains the intrinsic patch utility (i.e. the maximum potential utility of a patch, maxU[p]). We assume the accuracy of the reference memory to be maximal just after a visit of a patch, but to decline due to increasing uncertainty caused by memory decay (i.e. forgetting). The second mechanism controls the motivation to move away from recently visited patches: the working memory ($M_W[p]_t$), which stores the recency of the last visit. The strength of the working memory is maximal (~ 1) when the animal leaves the patch and decreases thereafter towards zero with the time elapsed since its last visit.

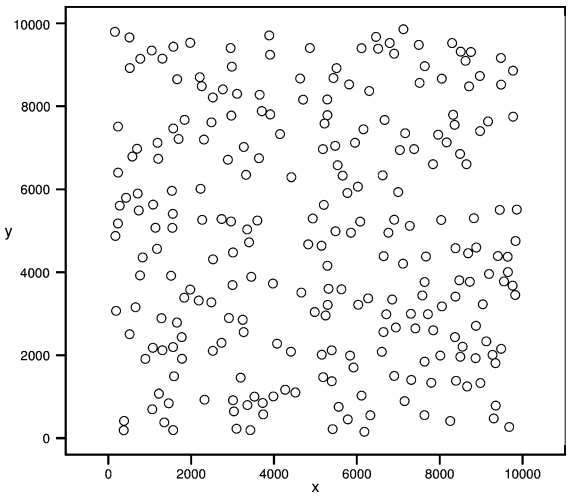

Figure 1. The simulated environment: 250 patches (radius = 106 units) on a landscape of 10 000 × 10 000 units.

For both memory types the variable memory strength for each patch ($M_R[p]_t$ and $M_W[p]_t$) can be modeled using a logistic model with negative slope. Such a function is loosely suggested by comparing the change of revisit probabilities with time in three different vertebrates (flower bats *Glossophaga soricina*, marsh tits *Parus palustris* and rufous hummingbirds *Selasphorus rufus*, reviewed by Winter and Stich 2005). Each memory type has its own characteristic decay rate, for the working and reference memory, respectively: r_W and r_R; the values of both parameters changed between simulations (Table 1). The upper and lower boundaries for the memory strength of a patch were respectively: 0.999 and 0.001, for both memory types.

$$M_R[p]_{t+1} = M_R[p]_t - r_R \times (1 - M_R[p]_t) \times M_R[p]_t \quad \text{and}$$

$$M_W[p]_{t+1} = M_W[p]_t - r_W \times (1 - M_W[p]_t) \times M_W[p]_t \tag{2}$$

The perceived patch utility is a combination of both memory types, i.e. the stored intrinsic patch utility (which is the intrinsic patch utility multiplied by the memory accuracy: $\text{maxU}[p] \times M_R[p]_t$) reduced to compensate for

the perceived recency of the last visit ($M_W[p]_t$). The perceived patch utility is divided by the travel distance to account for the fact that there is a cost of traveling towards the patch. This cost will increase with increasing travel distance; therefore the patch value (V'[p]t, Eq. 3) is the perceived patch utility divided by the travel distance (D[p]t)

$$V'[p]_{t+1} = \frac{(1 - MW[p]_{t+1}) \times MR[p]_{t+1} \times \max U[p]}{D[p]_t} \quad (3)$$

This solution is similar to Mitchell and Powell (2004). We used, however, the distance between each patch and the animal's position at time t, whereas Mitchell and Powell (2004) used the distance between the patches and the home-range center. The patch values are rescaled (V[p]t) to sum to one (Eq. 4).

$$V[p]_{t+1} = \frac{V'[p]_{t+1}}{\sum_{p=1}^{n} V'[p]_{t+1}} \quad (4)$$

The patch value (V[p]t) is the length of the attraction vector for the patch. The resultant attraction vector ($\vec{v}_t$) is the weighted sum of all the directions towards the patches ($\vec{d}$[p]t: unit vectors), weighted for the patch value (V[p]t). In other words, the resultant attraction vector ($\vec{v}_t$) is the sum of the attraction vectors for all patches. In addition to the attraction of patches, the resultant attraction vector also accounts for directional persistence, which is added as the previous direction ($\vec{r}_t$) weighted for the strength of the directional persistence (cor; it equals zero for the uncorrelated biased random walk). Thus the resultant attraction vector ($\vec{v}_t$) is given as:

$$\vec{v}_{t+1} = (1 - cor) \times \sum_{p=1}^{n} \{V[p]_{t+1} \times \vec{d}[p]_t\} + cor \times \vec{r}_t \quad (5)$$

Each movement step in our simulations has a fixed length and its direction drawn from a wrapped normal distribution (i.e. the circular equivalent of a classical normal probability distribution obtained by 'wrapping' a normal distribution around a circle), which is centered on the direction of the resultant attraction vector ($\vec{v}_t$) and has a variance proportional to the length of this vector ($\mu = \text{atan2}(\vec{v}_t), \sigma = -2 \times \log(|\vec{v}_t|)$). By making this variance proportional to the strength of the resultant attraction we modeled decision uncertainty by the animal. If the strength of attraction is maximal (i.e. close to one) the distribution is very narrow and the animal has a high probability to follow the direction of the attraction, whereas when the attraction strength is weak (i.e. close to zero) the distribution is close to uniform and the animal may go in any direction. It is worth noting that the indecisiveness between equally valued patches decreases due to two positive feedback mechanisms. By moving in the direction of one patch the distance to that patch decreases, thus its value will increase, and also the directional persistence in the movement leads to an increased probability to continue moving in the direction of that patch. After the direction is drawn from the wrapped normal distribution, the animal moves in that direction until the first patch is met, or until it reaches the step length value.

In this model we focus on inter-patch movements, thus once within a patch the animal no longer moves. The utility of a patch depletes after a certain time, but does not show any depression before depletion. As discussed above, this simplifies the model, because the optimal residence time for the animal is to stay until the patch is totally depleted (Stephens and Krebs 1986), after which the animal resumes its inter-patch movements.

Simulation and model analysis

We replicated 50 times the release of a single forager (thus foragers behaved independently) at a random location within the center square (size = 1000 × 1000 units) of the landscape. Each replicated forager was simulated for 5000 time steps. The forager could move outside the 10 000 × 10 000 unit landscape, but patches were constrained to that landscape. Using this approach we solved problems associated with two common alternatives, a closed environment and a torus. The former has boundary effects and methods for home-range calculation have not been developed for the later. Given the use of memory and learning in this model, we allowed for an initial transition ('learning') phase of 500 time steps. Biologically, this corresponds to the focal animal learning about its environment. Consequently, this transition phase was removed from the analysis of the simulated foragers' space use patterns.

We first investigated whether the inclusion of memory gives rise to a stable home range (i.e. a restricted area over time). We estimated the home range using a minimal convex polygon including 95% of the locations (known as MCP95; White and Garrott 1990). We preferred this method to kernel utilization distribution methods that are currently recommended for empirical studies of home-range size (Börger et al. 2006, Fieberg 2007) for two main reasons. First, Moorcroft and Lewis (2006) demonstrated recently that MCP95 is a useful tool to identify emergent home-range patterns in mechanistic space use simulation models (the size of MCP95 stabilizes in time for a 'return-to-origin' home-range model). Second, diffusion by a random walk leads to a range size that increases to infinity; therefore the probability of use for each pixel decreases towards zero. The limited number of decimal positions used by computers can lead to major difficulties in calculating home-range size for random walks over long time periods using kernel utilization distributions. We repeated the analysis using a fixed-kernel home-range estimator (excluding the cases where no estimation could be obtained). As expected, the results are even stronger, as MCP-based home-range estimators are extremely sensitive to outlying movements (Börger et al. 2006). In conclusion, for the specific case of identifying emergent home-range patterns in space use simulation models, like in this paper, using MCP95 estimators provide a convenient and robust approach.

In the literature on home ranges various methods have been proposed to assess the stability of a home range. Cooper (1978) proposed the overlap between consecutive home ranges to measure the temporal stability of home ranges. We used Cooper's method by splitting the locations

of the simulated trajectories into two parts, the first- and the second-half of each trajectory. Thereafter, we measured the overlap between these two home ranges. We additionally determined the overlap using also the volume of intersection (Millspaugh et al. 2004) of the kernel utilization distributions (Worton 1995) estimated using the locations from both halves of the trajectory. The results were highly correlated to those obtained using the overlap of MCP's ($r = 0.99$). Therefore, we restricted further analyses and discussion to the results using MCP95.

A direct assessment of the temporal stability of the home range is obtained by directly measuring the change of the total area covered with time (TAC[t]; Moorcroft and Lewis 2006). Using the MCP95, we calculated the TAC[t] including locations from $t = 1$ to $t = T$ (the interval between consecutive t's was 25 steps for reduced calculation time, thus we calculated home-range size at 180 different intervals). If a home range is bounded, then, after an initial increase in size when the animal moves through new areas, we expect the home range to stabilize as the animal starts moving back towards previously visited ('familiar') patches. Such behavior should result in a saturation curve of the TAC[t]. For an explicit assessment of the saturation properties of the curve we compared the fit of three biological models to the TAC[t] data: a linear ($TAC[t] = a + b \times t + \varepsilon$), a power ($TAC[t] = a \times t^b + \varepsilon$; with $b < 0.95$) and a saturation ($TAC[t] = \{a \times t/[b + t]\} + \varepsilon$) model (i.e. Michaelis–Menten saturation). These three functions represent the basic expected behavior of TAC[t]. Random walk models show a linear increase of TAC with time. According to Gautestad and Mysterud (1993, 1995) who predicted home ranges to show a power function, the TAC[t] should increase with the square root of time. Stable home ranges, however, should show a saturation of the TAC[t] over time, the b-parameter of this model providing the size of the area where the stabilization occurs (i.e. the home-range size). In the following, we will refer to these functions capturing the relationship between TAC[t] and time as the 'TAC[t]-models'.

Our model critically depends on the rate of change (r_W and r_R) of the two memory processes, because the direction of the movement is governed by the balance between both processes (M_W and M_R; Eq. 2, 3). We first assessed if and which rate combinations lead to a stable home range. To assess the sensitivity of the stable home range (A) to changes in the memory processes, we performed a regression analysis on the size of the stable home range (i.e. the b-parameter in the saturation model) using both memory process rates (r_W and r_R) as predictors (the process rates 0 and infinity were replaced by 1×10^{-5} and 10, respectively, to allow model fitting).

After having determined the memory rate combinations that gave rise to a home range, we performed a sensitivity analysis to assess the robustness of the results to changes in the model parameters: degree of directional persistence, step length, patch renewal rate and depletion rate (parameter values in Table 1). We investigated the effect of changing parameter values on the TAC[t]-model selection and using regression analysis we determined the effect of a one unit increase of parameter value on home range size (i.e. the regression slope). Thereafter we investigated how TAC over the whole simulation (i.e. $TAC[t = T]$) and mean acquired utility by the animal changed with the memory rates and for each of the three TAC[t]-models. An animal obtains utility from spending time in a non-depleted patch. The mean utility acquired over the simulation is measured as the total amount of 'utils' an animal obtained divided by the number of time steps. For $TAC[t = T]$ and mean acquired utility, we first investigated their sensitivity to changes in process rates of working and reference memory (i.e. r_W and r_R). We assessed the sensitivity using linear regression and determined the relative contribution of changes in process rate of working and reference memory to changes in both measures. We investigated the relationship between the $TAC[t = T]$ and mean acquired utility and the TAC[t]-models using box-plots.

For TAC[t]-model selection we used the information theoretic approach (AIC, Burnham and Anderson 2001). As is generally the case with analyses of the large number of data generated by simulations (Mitchell and Powell 2004) the differences in AIC values (ΔAIC) between models were invariantly very large. All simulations and analyses were done in R 2.5.0 (R Development Core Team 2005, the sp ver. 0.9), CircStats (ver. 0.2) and adehabitat (ver. 1.6, Calenge 2006) packages for spatial analysis, circular statistics, and home-range estimation, respectively. Model fitting was performed using Mathematica ver. 5.0.

Results

We developed a mechanistic home-range model using a biased correlated random walk (BCRW) approach. The simulated animal tracks a dynamic resource landscape using a biologically plausible two-part memory system composed of a reference- and a working memory. Both methods for determining home-range stability (i.e. the method determining home-range overlap between the first and second half of the simulated trajectory, and the method modeling the temporal dynamics of the total area covered, TAC[t]) showed that, depending on the decay rates of the working and reference memory, home ranges can emerge from a BCRW. Interestingly, the emergence of a home range leads also to more efficient resource use. We now present these results in detail.

Emergence of a home-range pattern

Different combinations of memory decay rates gave rise to a saturation model for TAC[t], i.e. led to the emergence of a stable home range (Fig. 2, 3). These results were confirmed by measuring the overlap between the first and second half of each simulated trajectory for assessing home-range stability (Fig. S1 in Supplementary material Appendix 1). In addition, as expected the three TAC[t]-models showed important differences in overlap (Fig. 4a). In the simulations where the linear function fitted best the TAC[t], the overlap between the first and second half of the trajectories was rather low ($X \pm SE$: 0.26 ± 0.0086), whereas in the case of both power and saturation models overlap was high (respectively: $X \pm SE$: 0.82 ± 0.026 and 0.85 ± 0.011).

We can see (Fig. 3) that simulations where the working memory has a faster process rate than the reference memory

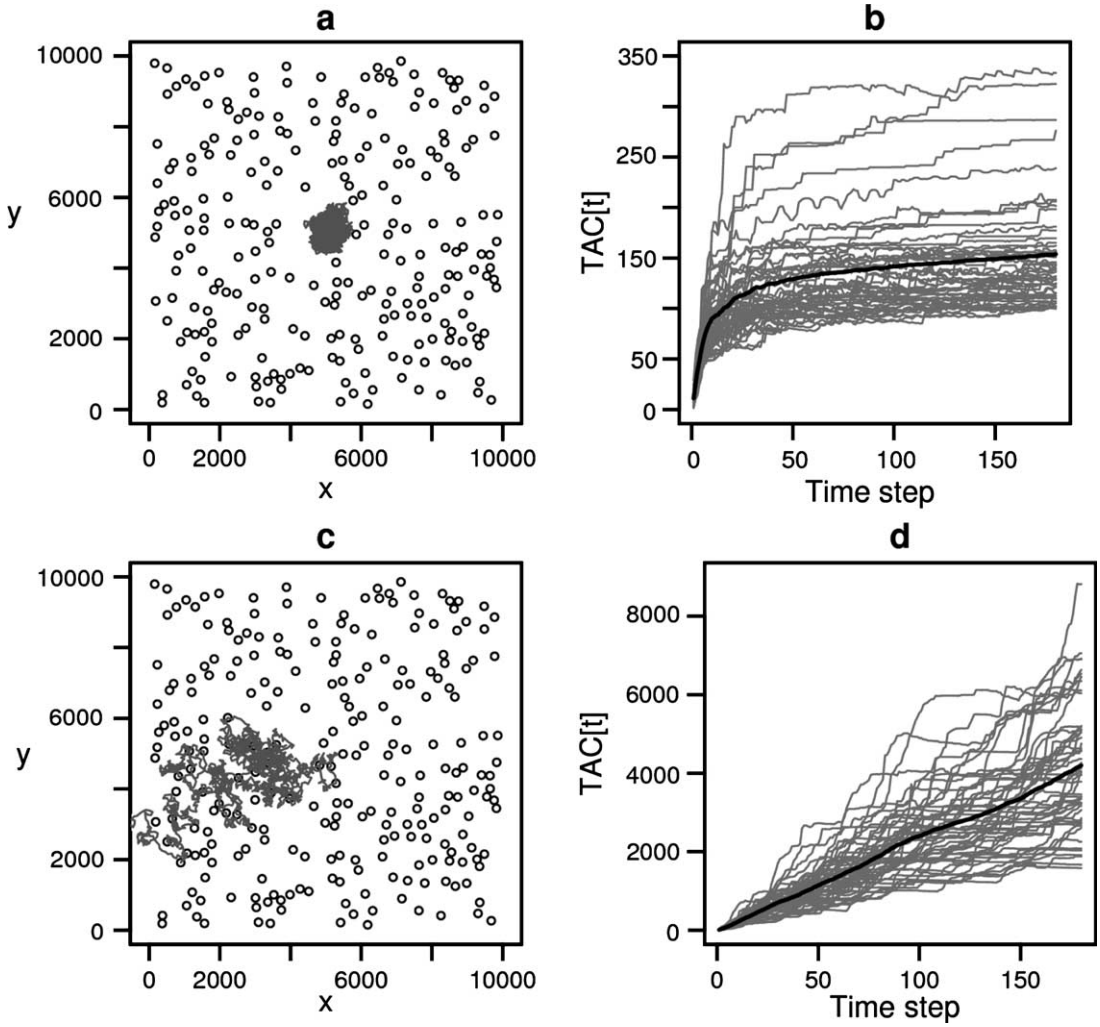

Figure 2. The upper panels (a and b) result from a simulation involving a stable home range (the decay rates for the reference and working memory are $r_R = 0.0001$ and $r_W = 0.01$, respectively). (a) shows one individual to illustrate the space use in this simulation and (b) shows how the total area covered (TAC[t]) changes with time for all individuals (in grey) and for the mean individual (in black). The lower panels (c and d) result from a simulated random walk without memory (the decay rates for both memory types are 'infinitely' large). (c) displays the case of an individual for illustration and (d) shows the change of the TAC[t] with time for all individuals (in grey) and the mean individual (in black).

($r_W > r_R$) are dominated by both saturation- and power-functions for TAC[t]. The reverse is true for simulations where the process rate of the reference memory is faster than that of the working memory ($r_W < r_R$), these are dominated by diffusion models (i.e. linear functions). However, this separation is not absolute. The number of simulations with saturation or power functions with slower working than reference memory rates was sizable, especially for slow reference memory process rates.

Sensitivity analysis

The robustness of home-range emergence was evaluated using a range of different values for each parameter (Table 1). None of the parameters changed the best fitting model for TAC[t], except for the degree of directional persistence ('cor' in Eq. 4). For the directional persistence, only values of 0.2 and 0.4 supported a saturation model, all other values supported a power relationship in the TAC[t] (the power exponent b increased with the correlation: 0.23, 0.32, and 0.46 for, respectively, cor = 0, 0.6, and 0.8; cor = 0.99 had model fitting problems, but visually also showed a power-relationship, Fig. S2 in the Supplementary material Appendix 1). The other parameters (i.e. step length, depletion rate and patch replenishment rate) did not change the saturation model from receiving most support.

Home-range size, instead, was strongly affected by changes in all parameter values (Fig. 5). Home-range size increased with larger step lengths (slope $\pm$ SE: 2.43 ± 0.055; $R^2 = 0.99$), higher intake rates (slope $\pm$ SE: 0.020 ± 0.0086; $R^2 = 0.63$) and lower patch replenishment rates (slope $\pm$ SE: $= -54 \pm 8.9$; $R^2 = 0.92$). Similarly, the total area covered over the whole simulation (i.e. TAC[t = T]) increased with increasing directional persistence (slope $\pm$ SE: $= 1006 \pm 400$; $R^2 = 0.68$; Fig. 5d). Note that, as mentioned above, not all directional persistence values gave rise to a stable home range. Therefore, we used TAC[t = T] instead of home-range size to evaluate the

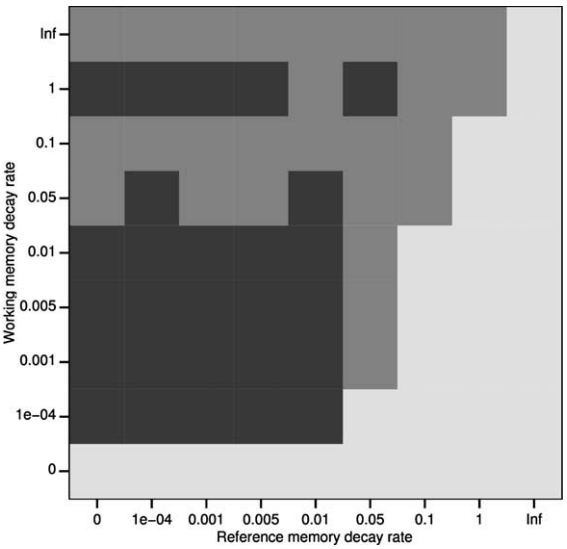

Figure 3. Best fitting models for different combinations of both memory parameters. Three models were fitted (See main text for details): a linear ($ax+b$; in white), a power (ax^b; in grey) and a saturation model ($ax/(b+x)$; in black).

effect of different values of directional persistence on the simulated space use patterns.

Total area covered during the whole simulation

For simulations for which we observed a stable home range the size of this home range (A) was rather insensitive to the rate of the reference memory ($\log(r_R)$; $\beta \pm$SE: -1.78 ± 3.20; $R^2 = 0.004$), whereas it was very sensitive to changes in the working memory rate ($\log(r_W)$; $\beta \pm$SE: -52.11 ± -18.84; $R^2 = 0.92$). Thus, the size of the stable home range (A) is largely determined by the working memory. This insensitivity to changes in the reference memory was, however, not true for the TAC[t = T] for all simulations together (i.e. including all combinations of memory process rates for both working and reference memory; Fig. 6). The TAC[t = T] turned out to be sensitive to changes in the rate of both working ($\log(r_W)$; $\beta \pm$SE: -459.22 ± 77.84; $R^2 = 0.21$) and reference memory ($\log(r_R)$; $\beta \pm$SE: 569.34 ± 77.84; $R^2 = 0.32$). The diffusion models (i.e. those simulations where linear functions received the highest support for the TAC[t]) showed a much higher TAC[t = T] (X ± SE: 3630 ± 213) than both power functions (X ± SE: 115 ± 30) and saturation functions (X ± SE: 151 ± 13) (Fig. 4b). Accordingly, TAC[t = T] and home-range overlap show a strong negative correlation ($r = -0.92$).

Mean acquired utility dynamics

The mean acquired utility is the mean utility a simulated animal obtains at each time step, calculated by dividing the total utility intake by the total number of time steps. The mean acquired utility for stable home ranges was rather insensitive to changes in the rate of the reference memory ($\log(r_R)$; $\beta \pm$SE: -2.21 ± 48.92; $R^2 = 0.001$), but sensitive to changes in the working memory rate ($\log(r_W)$; $\beta \pm$SE: -161.49 ± 42.06; $R^2 = 0.37$). Considering all simulations,

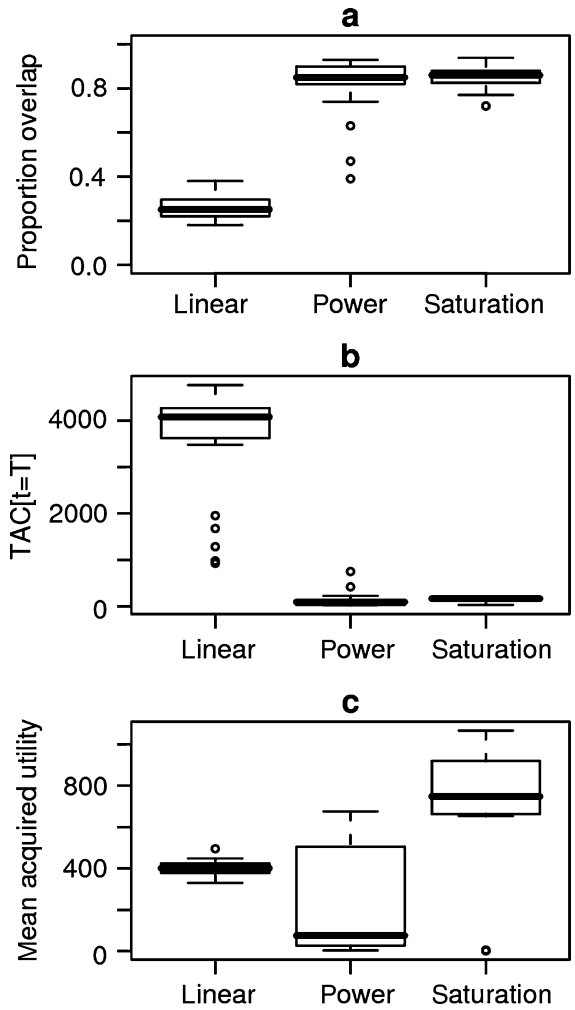

Figure 4. Boxplots of the proportion overlap, the total area covered for the whole trajectory (TAC[t = T]) and mean acquired utility for the three different TAC[t]-models (see main text for further explanation). Shown from left to right: first the linear model, then the power model and finally the saturation model. The upper panel (a) shows the proportion overlap between the first and second half of the simulation, the panel in the middle (b) the TAC[t = T] calculated as the MCP95 for the whole trajectory and the bottom panel (c) shows the mean acquired utility, which is the total utility the forager consumes during the simulation divided by the number of time steps.

the mean acquired utility rate remained most sensitive to changes in the decay rate of the working memory ($\log(r_W)$; $\beta \pm$SE: -87.49 ± 16.39; $R^2 = 0.26$), but was also somewhat sensitive to changes in the rate of the reference memory ($\log(r_R)$; $\beta \pm$SE: -35.91 ± 16.39; $R^2 = 0.05$; Fig. 7). The relation between acquired utility and process rates of both memory processes was markedly non-linear (Fig. 7). Highest acquired utilities occurred with parameters representing a low process rate for the reference memory and intermediate rates for the working memory. The mean acquired utility was markedly different for both saturation and power functions (Fig. 4c). The saturation models showed higher acquired utility (X ± SE: 674 ± 67) than both linear models (X ± SE: 403 ± 6.3) and power models (X ± SE: 198 ± 47), with the latter having the lowest mean acquired utility.

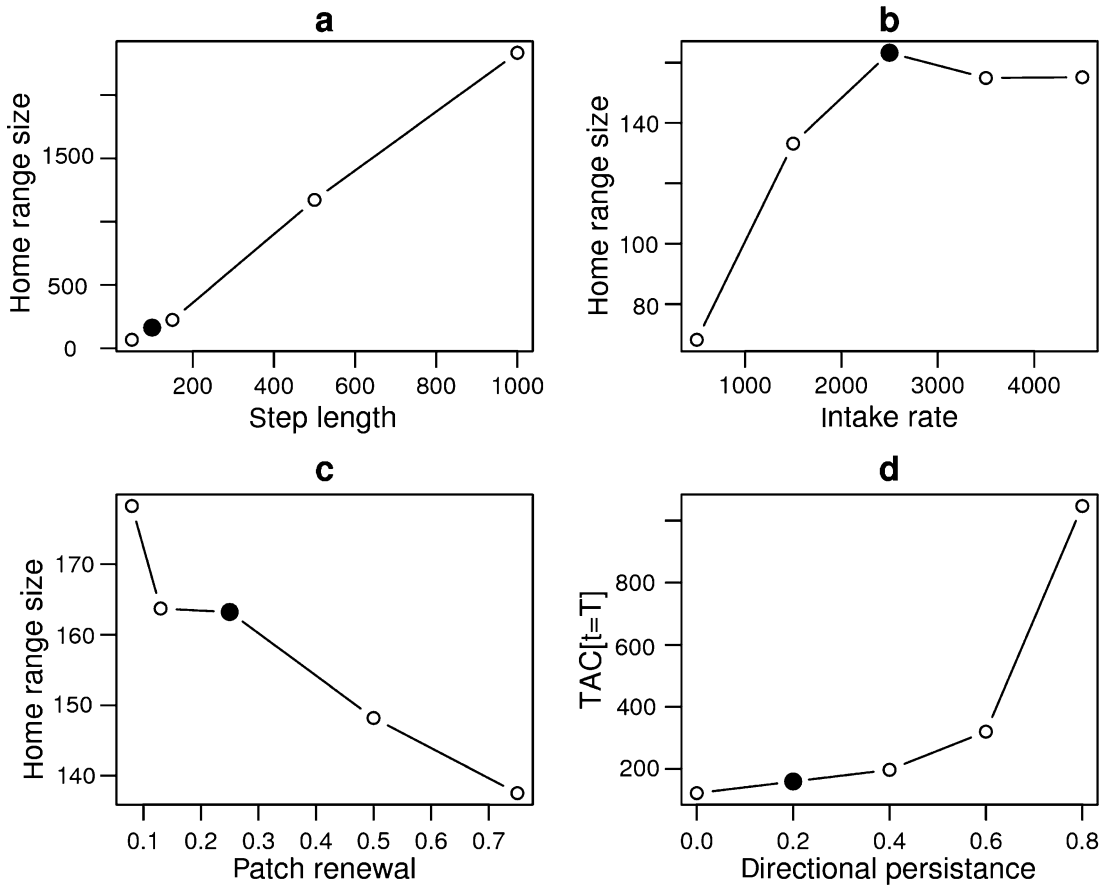

Figure 5. Sensitivity of home-range size to changes model parameter values. The filled black circle shows the default values, the open circles show the other values in the range considered (Table 1). (a) shows the sensitivity to changing step length values, (b) intake rate, (c) patch replenishment speed and (d) to changes in the degree of directional persistence. Note the change in the *y*-axis in (d): for some values of directional persistence no stable home range emerged, as an alternative for home-range size the total area covered over the whole trajectory (TAC[t = T]) is reported.

The relationship between mean acquired utility and TAC[t = T] was non-linear. Small TAC[t = T]s, generally characterized by power TAC[t] functions, had the lowest acquired utility (Fig. 8). For somewhat larger TAC[t = T]s, mostly supporting a saturation function, we found the maximum acquired utility. The largest TAC[t = T]s, typically a linear function, showed an intermediate acquired utility.

Discussion

Using different methods to assess the emergence of home ranges from a biased correlated random walk, we showed that including memory processes can give rise to a variety of space use patterns, from diffusion to the high stability corresponding to the concept of the home range (Cooper 1978). To our knowledge, we provided here for the first time a mechanistic home-range model based on a correlated random walk that recreates home-range patterns without requiring the assumption of territoriality or central place foraging as in all previous mechanistic home-range models (Börger et al. 2008).

Two mechanisms are required to lead to temporally stable home ranges: one to motivate the animal to move away from an attractor (the working memory), and another to motivate the animal to return to the attractor (the reference memory). The absence of a reference memory (i.e. r_R = infinity) leads to diffusion (Fig. 3). Whereas, the absence of a working memory (i.e. r_W = infinity) results in the absence of inter-patch movement; the animal is then essentially moving in and out a single patch (see the extremely small TAC[t = T] in Fig. 6).

When a home range emerges, both mechanisms lead to two different dynamics depending on spatio-temporal scale. At larger scale, the emergence of a home range results in relative immobility, whereas within the home range there is movement between patches. The emergence of stable home ranges occurs mostly when the decay rate of working memory is relatively larger than that of reference memory (Fig. 3). This result is congruent with the literature. The working memory is a relatively short-term memory, whereas the reference memory is a long-term memory (Howery et al. 1999).

The memory parameter combination that resulted in the highest acquired utility had an intermediate working memory and a low reference memory process rate. This maximum was relatively robust to changes in process rate of the reference memory (for memory rate combinations that resulted in stable home ranges). Utility is obtained only

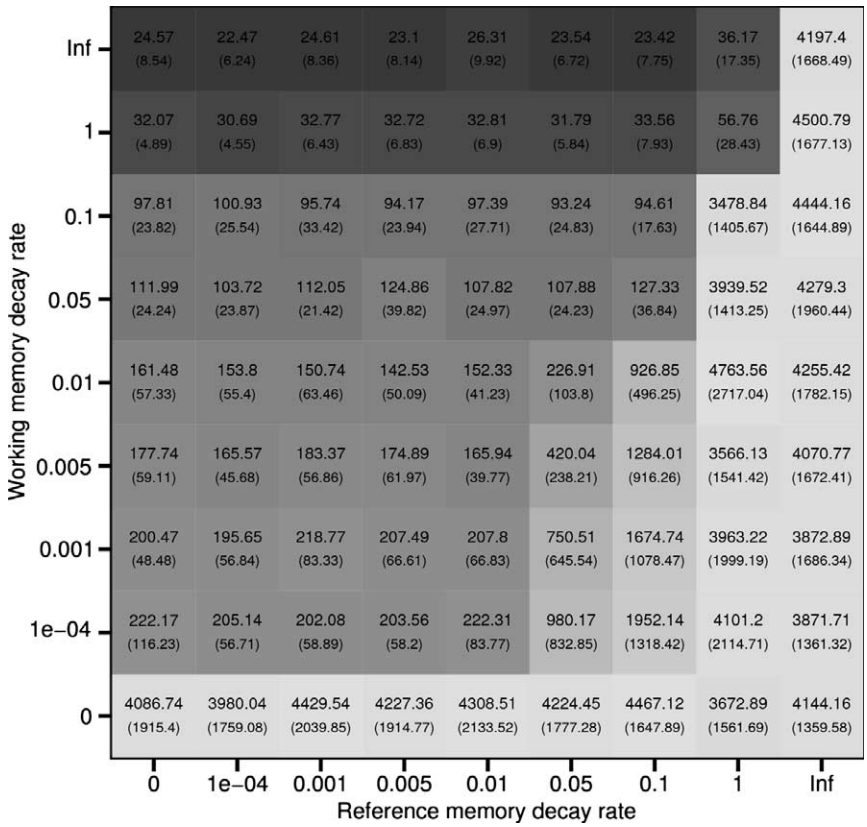

Figure 6. Mean (SE) total area covered for the whole tracectory (TAC[t=T]) as fuction of the reference and working memory decay rates. This area is calculated by the MCP95 after 5000 time steps. For a better reading of the figure, we used the natural logarithm for the color coding (darker cells are smaller areas, whereas the parameter combinations that lead to larger areas are light). The graph shows that within a wide range of values of memory decay the TAC[t = T] stays relatively small (TAC < 300). The transition between small and large TAC[t = T] is quite abrupt and often close to the diagonal where the working memory decay becomes smaller than the reference memory decay.

within patches and our model does not contain any intra-patch movements. Therefore acquired utility is a good synthetic measure for the efficiency of the animal, because it combines both the costs and the benefits associated with movement in our simulations.

The higher efficiency of animals that limit their movement within a sufficiently large home range as compared to animals staying in a too small area or diffusing (i.e. that have no home range) is an interesting result. Individuals staying in too small areas seem to be more penalized than those ranging over a too large area. The advantage of moving away from depleted areas might not come as a surprise. However, the higher efficiency of animals with a stable home range over ones wandering at random is far from trivial. As discussed above, to avoid backtracking the working memory is necessary, whereas the reference memory is needed to return to previously visited sites. Our results suggest that such a two-part memory system not only gives rise to a stable home range, but also has an advantage over animals lacking either component. This offers interesting new directions for our thinking about the evolution of home-range behavior, which might emerge as a consequence of spatial memory. Nonetheless, it is premature to conclude from our study that a two-part spatial memory that gives rise to a stable home range leads also to optimal use of resources in a predictable heterogeneous environment. Our comparison was restricted to random walks with two memory processes differing in process rates. Future research should compare this movement model with other search models like straight-line movement or systematic searching (Bell 1991).

The emergence of a stable home range was robust to changes of most model parameters other than the memory rates (i.e. step length, patch depletion rate, patch renewal rate, and directional persistence). The size of this stable home range, however, changed considerably with the parameter values. Interestingly, the sensitivity of home-range size to these parameter values might be used to understand both intra- and inter-specific variation in home-range size. Inter-specific variation in home-range size has been related to changing energetic requirements due to body mass differences (Harestad and Bunnell 1979). However, the underlying mechanism is lacking. Body mass is related to both step length (Pontzer 2007) and depletion or intake rate (Shipley et al. 1994), both parameters are in our simulations related to home-range size. However, this relationship becomes more complex as the environment (i.e. patch size and patch replenishment) is likely to change with body mass as well (Price 1983). Nonetheless, the model presented here seems promising providing more insight into the allometric relationships of home-range size.

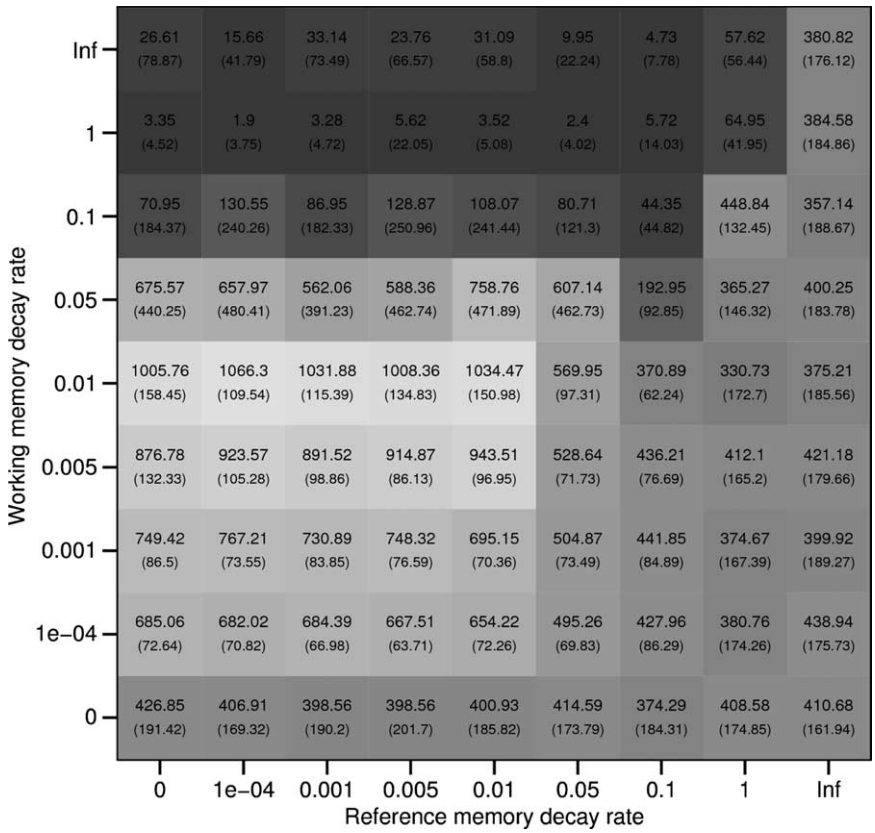

Figure 7. Mean (SE) intake as a function of the reference and working memory decay rate. The highest intakes occur at low decay rates for the reference and at intermediate values for the working memory.

An increasing home-range size with increased depletion rate or decreased patch renewal rate also is consistent with empirical findings within single species. Home-range size generally increases with decreasing habitat quality (Anderson et al. 2005, Saïd et al. 2005). Lowered habitat quality can be observed in changes of each of three habitat features: higher patch depletion rate (i.e. decreased patch utility or patch size), slower patch renewal, and lower patch density. We tested the effect of the first two components, both lead indeed to the observed changes in home-range size (see below for a discussion of patch distribution).

The only other parameter influencing the emergence of a stable home range is the degree of directional persistence of the correlated random walk. There is a direct tradeoff between the attraction vector of the environment and the directional persistence vector (Eq. 2). Thus, with increasing directional persistence the influence of the environment decreases. This might explain why high levels of directional persistence lead to less stable home ranges.

The emergence of a stable home range in our simulations turned out to be rather robust to changes of the parameter values. Still, we did not investigate the representation of environmental heterogeneity and the form of the patch depletion function on the formation and stability of home ranges. In our simulation we used distinct patches in Cartesian space. An alternative representation of spatial heterogeneity would be to use pixels to create a gradient in continuous space (Mitchell and Powell 2004). However, the major advantage of a patch-based representation is the straightforward determination of the attractors. By considering each pixel as a patch, as done by Mitchell and Powell (2004), our model easily can be applied on pixel-based landscapes (previous simulations in such a pixel landscape showed similar general results, Van Moorter unpubl.).

The spatial location of the patches in our simulated environment did not change and patch replenishment was deterministic resulting in a predictable environment. The emergence of a home range in our simulation, however, does not depend as such on the dynamics of the environment rather than on the cognitive dynamics of the animal. As long as the animal continues to return to previously visited patch locations, a home range can emerge regardless of whether the patch is still there. Nonetheless, it is probably unlikely that an animal behaving in this way will be more efficient than an animal wandering at random unless the probability of finding a patch at a familiar location is higher than random. In addition, future research should investigate how the emergence and the size of the home range are influenced by variation in spatial heterogeneity and predictability. Mitchell and Powell (2004) identified interesting relationships between the spatial distribution of resources and home-range size (e.g. home ranges in highly clumped environments were smaller than in environments with more dispersed resources). Unfortunately, however, their model was not movement-based.

To simplify the patch-leaving rule in our simulations we opted for patch depletion without patch depression. Such a gain function might be of only limited realism (Stephens and Krebs 1986). Other gain functions would lead to

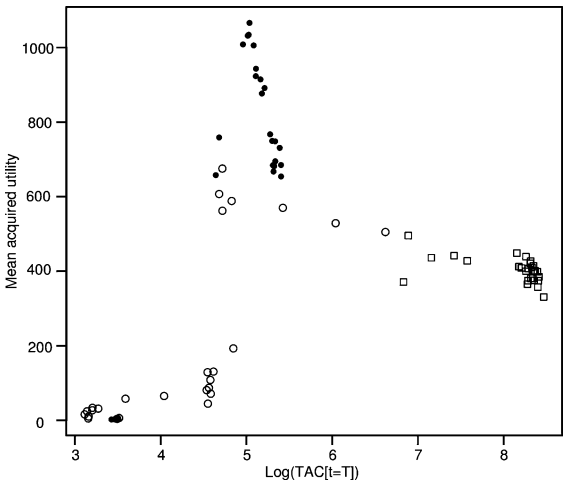

Figure 8. Relationship between mean acquired utility and total area covered during the whole trajectory (TAC[t = T]). The different TAC[t]-models are represented by different symbols: filled circles for saturation, open circles for power and squares for linear models. The TAC[t=T] is log-transformed for an improved readability of the x-axis.

different patch residence times or different patch renewal times (Possingham and Houston 1990). However, we have shown that patch residence time, which in our model is influenced by depletion rate, and patch renewal time have no effect on the emergence of a stable home range. Therefore the emergence of a stable home range is unlikely to depend upon the specific shape of the gain function, although the size of the home range should be affected as we have shown.

The use of attractors (i.e. patches), with a force of attraction that changes in time due to the dynamics of working and reference memory creates a dynamic attractor field in which the animal moves. Such a dynamic attractor field is strongly related to the 'active walker' paradigm (Lam 1995). One can envisage here the emergence of a general animal movement model based on movement in a dynamic attractor field, whose form and dynamics allows for the modeling of a multitude of biological models, like social animals by including conspecific attraction (Dumont and Hill 2001, Couzin et al. 2002, Haydon et al. 2008). In our model attractors only exerted a positive attraction. Negative attraction, on the other hand, can lead to the repulsion from sites having a negative utility for an animal (e.g. high in predation risk, void of resources, or containing the scent marks of a rival pack). In this framework the return-to-origin rule of a central place forager is a simple attractor field with only one attractor (i.e. the origin). The attractors (or repulsors) in the field can vary not only in spatial position and average attractivity, they can also show different temporal dynamics (i.e. utility function) depending on the biological reality they represent. The only requirement for the utility function is that it has to decrease with residence time (recall that utility depends on both the environment and the animal, it is thus influenced also by the animal's state). Otherwise the motivation for movement is lacking, which will result in a stasis rather than movement.

In conclusion, the model presented here allows for the simulation of stable home ranges using the random walk approach, which is widely used to model animal movements (Turchin 1998). The model is more general than previous home-range models (reviewed by Börger et al. 2008) and is applicable for animals with more than one point of attraction (i.e. multi-nuclear home ranges). Thus, no assumption of central place foraging is made. Two processes, which we relate to memory, are needed: one pushing the animal away from an attractor, the other attracting the animal back to the attractor; the first one operating at a faster time scale than the later one leads to stability. Another interesting finding is the higher efficiency of simulations showing a stable home range than simulations showing diffusion or relative stationarity.

Acknowledgements – BVM was financially supported by a research grant from the French government. DV was funded by a NSERC Industrial Scholarship in collaboration with Weyerhaeuser. We also thank the ANR program 'Mobilité' for fincancial support. The paper was enhanced by constructive comments from R. Powell and H. Possingham on a previous version of the manuscript.

References

Anderson, D. P. et al. 2005. Factors influencing female home range sizes in elk (*Cervus elaphus*) in North American landscapes. – Landscape Ecol. 20: 257–271.

Arvisais, M. et al. 2002. Home range and movements of a wood turtle (*Clemmys insculpta*) population at the northern limit of its range. – Can. J. Zool. 80: 402–408.

Beecham, J. A. and Farnsworth, K. D. 1998. Animal foraging from an individual perspective: an object orientated model. – Ecol. Modell. 113: 141–156.

Bell, W. J. 1991. Searching behaviour. The behavioural ecology of finding resources. Animal behaviour series. – Chapman and Hall.

Börger, L. et al. 2006. Effects of sampling regime on the mean and variance of home range size estimates. – J. Anim. Ecol. 75: 1393–1405.

Börger, L. et al. 2008. Are there general mechanism of animal home range behavior? A review and prospects for future research. – Ecol. Lett. 11: 637–650.

Bovet, P. and Benhamou, S. 1988. Spatial analysis of animals' movements using a correlated random walk model. – J. Theor. Biol. 131: 419–433.

Brown, M. F. et al. 1997. The existence and extent of spatial working memory ability in honeybees. – Anim. Learning Behav. 25: 473–484.

Burnham, K. P. and Anderson, D. R. 1998. Model selection and inference: a practical information-theoretic approach – Springer.

Burt, W. H. 1943. Territoriality and home range concepts as applied to mammals. – J. Mammal. 24: 346–352.

Calenge, C. 2006. The package adehabitat for the R software: a tool for the analysis of space and habitat use by animals. – Ecol. Modell. 197: 516–519.

Charnov, E. L. 1976. Optimal foraging: the marginal value theorem. – Theor. Popul. Biol. 9: 129–136.

Cooper, W. E. Jr. 1978. Home range criteria based on temporal stability of areal occupation. – J. Theor. Biol. 73: 687–695.

Couzin, I. D. et al. 2002. Collective memory and spatial sorting in animal groups. – J. Theor. Biol. 218: 1–11.

Crook, D. A. 2004. Is the home range concept compatible with the movements of two species of lowland river fish? – J. Anim. Ecol. 73: 353–366.

Crump, M. L. 1986. Homing and site fidelity in a Neotropical frog, *Atelopus varius* (Bufonidae). – Copeia 1986: 438–444.

Daugherty, C. H. and Sheldon, A. L. 1982. Age-specific movement patterns of the frog *Ascaphus truei*. – Herpetologica 38: 468–474.
Don, B. A. C. and Rennolls, K. 1983. A home range model incorporating biological attraction points. – J. Anim. Ecol. 52: 69–81.
Dumont, B. and Hill, D. 2001. Multi-agent simulation of group foraging in sheep: effects of spatial memory, conspecific attraction and plot size. – Ecol. Modell. 141: 201–215.
Fagan, W. et al. 2007. Population and community consequences of spatial subsidies derived from central-place foraging. – Am. Nat. 170: 902–915.
Fieberg, J. 2007. Utilization distribution estimation using weighted kernel density estimators. – J. Wildlife Manage. 71: 1669–1675.
Foerster, C. R. and Vaughan, C. 2002. Home range, habitat use, and activity of Baird's tapir in Costa Rica. – Biotropica 34: 423–437.
Folse, L. J. et al. 1989. AI modeling of animal movements in a heterogeneous habitat. – Ecol. Modell. 46: 57–72.
Gautestad A. O. and Mysterud, I. 1993. Physical and biological mechanisma in animal movement processes. – J. Appl. Ecol. 30: 523–535.
Gautestad, A. O. and Mysterud, I. 1995. The home range ghost. – Oikos 74: 195–204.
Gautestad, A. O. and Mysterud, I. 2005. Intrinsic scaling complexity in animal dispersion and abundance. – Am. Nat. 165: 44–55.
Greenwood, P. J. and Harvey, P. H. 1982. The natal and breeding dispersal of birds. – Annu. Rev. Ecol. Syst. 13: 1–21.
Harestad, A. S. and Bunnell, F. L. 1979. Home range and body weight – a reevaluation. – Ecology 60: 389–402.
Haydon, D. T. et al. 2008. Socially informed random walks: incorporating group dynamics into models of population spread and growth. – Proc. R. Soc. Lond. B. 275: 1101–1109.
Heise, C. D. and Epperson, D. M. 2005. Site fidelity and home range of relocated gopher tortoises in Mississippi. – Appl. Herpetol. 2: 171–186.
Honig, W. K. 1978. Studies of working memory in the pigeon. – In: Hulse, S H. et al. (eds), Cognitive processes in animal behavior. Erlbaum, Hillsdale, NJ, pp. 211–248.
Howery, L. D. et al. 1999. Impact of spatial memory on habitat use. – Grazing Behav. Livestock Wildlife 70: 91–100.
Lam, L. 1995. Active walker models for complex systems. – Chaos Solitons Fractals 6: 267–285.
Martinoli, A. et al. 2006. Recapture of ringed *Eptesicus nilssonii* (Chiroptera, Vespertilionidae) after 12 years: an example of high site fidelity. – Mammalia 70: 333–335.
Millspaugh, Z. Z. et al. 2004. Comparability of three analytical techniques toassess joint space use. – Wildlife Soc. Bull. 32: 148–157.
Mitchell, W. A. and Lima, S. L. 2002. Predator-prey shell games: large-scale movement and its implications for decision-making by prey. – Oikos 99: 249–259.
Mitchell, M. S. and Powell, R. A. 2004. A mechanistic home range model for optimal use of spatially distributed resources. – Ecol. Modell. 177: 209–232.
Mitchell, M. S. and Powell, R. A. 2007. Optimal use of resources structures home ranges and spatial distribution of black bears. – Anim. Behav. 74: 219–230.
Mooney, K. A. and Haloin, J.R. 2005. Nest site fidelity of *Paraphidippus aurantia* (Salticidae). – J. Arachnol. 34: 241–243.
Moorcroft, P. R. and Lewis, M. A. 2006. Mechanistic home range analysis. – Princeton Univ. Press.
Moorcroft, P. R. et al. 1999. Home range analysis using a mechanistic home range model. – Ecology 80: 1656–1665.
Pettersson, L. B. and Brönmark, C. 1993. Trading off safety against food: state dependent habitat choice and foraging in crucian carp. – Oecologia 95: 353–357.
Pontzer, H. 2007. Effective limb length and the scaling of locomotor cost in terrestrial animals. – J. Exp. Biol. 210: 1752–1761.
Possingham, H. P. 1988. A model of resource renewal and depletion: applications to the distribution and abundance of nectar in flowers. – Theor. Popul. Biol. 33: 138–160.
Possingham, H. P. and Houston, A. I. 1990. Optimal patch use by a territorial forager. – J. Theor. Biol. 145: 343–353.
Price, M. V. 1983. Ecological consequences of body size: a model for patch choice in desert rodents. – Oecologia 59: 384–392.
Rhodes, J. R. et al. 2005. A spatially explicit habitat selection model incorporating home range behavior. – Ecology 86: 1199–1205.
Rodríguez, M. A. 2002. Restricted movement in stream fish: the paradigm is incomplete, not lost. – Ecology 83: 1–13.
Saïd, S. et al. 2005. Ecological correlates of home range size in spring-summer for female roe deer (*Capreolus capreolus*) in a deciduous woodland. – J. Zool. 267: 301–308.
Schaefer, J. A. et al. 2000. Site fidelity of female caribou at multiple spatial scales. – Landscape Ecol. 15: 731–739.
Shipley, L. A. et al. 1994. The scaling of intake rate in mammalian herbivores. – Am. Nat. 143: 1055–1082.
Solow, A.R. 1990. A note on the statistical properties of animal locations. – J. Math. Biol. 29: 189–193.
Spencer, S. R. et al. 1990. Operationally defining home range: temporal dependence exhibited by hispid cotton rats. – Ecology 71: 1817–1822.
Stamps, J. A. and Krishnan, V. V. 1999. A learning-based model of territory establishment. – Q. Rev. Biol. 74: 291–318.
Stephens, D. W. and Krebs, J. R. 1986. Foraging theory. – Princeton Univ. Press.
Switzer, P. V. 1997. Factors influencing the site fidelity of a territorial animal, *Perithemis tenera*. – Anim. Behav. 43: 865–877.
Tan, Z.-J. et al. 2001. "True" self-attracting walk. – Phys. Lett. A 289: 251–254.
Tan, Z.-J. et al. 2002. Random walk with memory enhancement and decay. – Phys. Rev. E 65.
Turchin, P. 1998. Quantitative analysis of movement: measuring and modeling population redistribution in animals and plants. – Sinauer.
Wang, M. and Grimm, V. 2007. Home range dynamics and population regulation: an individual-based model of the common shrew *Sorex ayaneus*. – Ecol. Modell. 205: 397–409.
Wiens, J. A. 1979. On competition and variable environments. – Am. Sci. 65: 590–597.
Weimerskirch, H. 2007. Are seabirds foraging for unpredictable resources? – Deep-Sea Res. II 54: 211–223.
White, G. W. and Garrott, R. A. 1990. Analysis of wildlife radiotracking data. – Academic Press.
Winter, Y. and Stich, K.P. 2007. Foraging in a complex naturalistic environment: capacity of spatial working memory in flower bats. – J. Exp. Biol. 208: 539–548.
Worton, B. J. 1995. Using Monte Carlo simulation to evaluate kernel-based home range estimators. – J. Wildlife Manage. 59: 794–800.

Supplementary material (available online as Appendix O17003 at www.oikos.ekol.lu.se/Appendix). Appendix 1.